

A Lattice Model for the Surface Segregation of Polymer Chains Due to Molecular Weight Effects

Arvind Hariharan and Sanat K. Kumar*

*Department of Materials Science and Engineering, Polymer Science Program,
The Pennsylvania State University, University Park, Pennsylvania 16802*

Thomas P. Russell

*IBM Research Division, Almaden Research Center, 650 Harry Road,
San Jose, California 95120*

Received August 30, 1989

ABSTRACT: The effects of polydispersity on the behavior of a polymer melt near a surface are considered in this work. To study these effects we have modeled an athermal polymer melt with a bimodal molecular weight distribution in the vicinity of a neutral surface in the spirit of the mean-field lattice treatments of Scheutjens and Fleer²⁰ and Theodorou.²³ The results of the calculations show that purely entropic effects cause the shorter chains in the system to partition preferentially to the surface. This partitioning becomes more pronounced with increases in the difference between the molecular weights of the chains. The concentration profile of the segments of any one species in the vicinity of the wall can be described by a hyperbolic tangent function with a single correlation length that is a simple function of the mixture composition and the radii of gyration of the two chains. Implications of these results on the surface tension and orientation of chain segments in the interface of a bimodal polymer melt are also examined.

1. Introduction

The behavior of polymers at interfaces has recently been studied in detail through computer simulations¹ and experiments.²⁻⁴ Systems of this type find applications at many levels of industrial practice, with the use of polymers as lubricants and as thin-film dielectrics being typical examples. Any polymer composite is made up of numerous interfaces formed due to the contact of a polymer with fillers dispersed within. The mechanical properties of these composites are determined by the nature of these interfaces.

Physically if one pictures polymer chains as random coils, then bringing these coils in contact with a solid surface (such as a filler) would decrease the conformational freedom, and hence the entropy, of these chains. The extent of the reduction in the entropy and the corresponding change in the interfacial free energy determines the nature of adhesion of the polymer to the substrate. Understanding of such situations to date has been restricted to model, monodisperse polymers in contact with idealized surfaces.¹ In practical situations, however, polydisperse polymers are used. If the melt is polydisperse, the entropic loss suffered by the longer chains in the vicinity of the surface, in the absence of any energetic interactions, would be greater than that for the shorter chains due to the restriction posed by connectivity of the chain segments. Thus, this argument suggests that the shorter chains would segregate to the surface in order to enable the system to reach a state of maximum possible entropy at equilibrium. One therefore expects the composition of the polymer close to the surface to be different from the bulk composition, with the difference becoming negligible at distances that determine the size of the interface.

It was shown by Anastasiadis et al.⁵ that the surface tension of a monodisperse polymer depends on its molecular weight, M , as $M^{-2/3}$. Thus, if there is substantial surface enrichment of the shorter chains from a polydis-

perse melt, one can expect a decrease in the surface tension and, hence, a significant change in the adhesion between polymer and substrate. The motivation for investigating the effect of polydispersity on the microstructure of the interface is to examine if entropic effects have any important consequences on its physical properties.

In the past, a variety of theories have been used to investigate related problems.⁶⁻¹⁹ Among the recent ones a comprehensive treatment was provided by Scheutjens and Fleer.²⁰ This theory, which was developed to model monodisperse polymer solutions in contact with an impenetrable, homogenous surface,²⁰⁻²² took into account many of the simplifying assumptions made by the older theories. Developed in the framework of a quasi-crystalline mean-field lattice model, it utilized the matrix procedure developed by DiMarzio and Rubin¹⁵ to evaluate the entropy of the confined polymer system. Further, energetic interactions between polymer-solvent, polymer-surface, and solvent-surface were also included in the formulation through the use of appropriate Flory interaction parameters.²⁰ Theodorou²³ subsequently extended this theory to model the behavior of monodisperse polymers in the vicinity of a solid surface.

The effects of polydispersity on the behavior of a polymer melt near a surface are considered in this work. To study these effects we have modeled an athermal polymer with a bimodal molecular weight distribution in the vicinity of a neutral surface (meaning that the surface has the same energetic interaction with any segment of the two different chain length species comprising the bimodal melt) in the spirit of the mean-field lattice treatments of Scheutjens and Fleer²⁰ and Theodorou.²³ It is emphasized that we only consider the segregation of chains due to entropic effects. The primary quantity that is considered is the concentration profiles of the segments of the shorter chains in the vicinity of the wall. Implications of these results on the orientation of chain segments in the interface and also the surface tension of a bimodal melt are also examined.

* Author to whom correspondence should be addressed.

2. Theoretical Development: Bimodal Melt

2.1. Formulation of the Partition Function. In the formulation of the partition function we follow closely the methodology used by Scheutjens and Fleer.²⁰ Consider a bimodal mixture of N polymer chains, n_1 of them with r_1 segments each and n_2 of them with r_2 segments each. All the molecules are assumed to be distributed over a lattice having M layers numbered sequentially, with 1 and M being the surfaces. Let each layer contain L lattice sites and every site be occupied by one segment only. Each lattice site is isodiametric, so that each site is approximately 4.5 Å on a side in the case of polyethylene. Since we have a polymer melt system, we assume complete lattice filling, a condition that can be expressed mathematically as

$$r_1 n_1 + r_2 n_2 = ML \quad (1)$$

Denoting the number of segments of the two different chains in any layer i by $n_{1,i}$ and $n_{2,i}$, respectively, we have

$$\Phi_{l,i} = n_{l,i}/L \quad l = 1, 2 \quad (2)$$

where $\Phi_{l,i}$ denotes the volume fraction of species l in layer i .

We label the segments comprising the two chains by $s_1 = 1, 2, 3, \dots, r_1$ and $s_2 = 1, 2, 3, \dots, r_2$. Any conformation c_i of a chain of length r_i can be denoted by $(1,i)(2,j) \dots (r_i,k) \dots (r_i,l)(r_i,m)$, implying that the first segment of the chain in this conformation is in layer i , the second in j , and so on. It should be recognized that this technique subdivides conformational space in terms of layer positions of the segments and is hence a very coarse grained description. For example, such a characterization would not preclude the back-stepping of a chain onto itself and also does not prevent the formation of closed loops. Corrections to overcome these errors can be made if one resorts to a more detailed depiction of chain conformations, as we have shown in another publication in a different context.²⁶ For this analysis we employ this crude description due to its inherent simplicity, and the extension of this formulation to account for more detailed conformational characteristics is deferred to a future publication.

The grand canonical partition function for this system is defined formally as

$$G = \sum Q(\{n_{c_1}\}, \{n_{c_2}\}, M, L, T) \exp(\mu_1 \sum_{c_1} n_{c_1}/kT) \times \exp(\mu_2 \sum_{c_2} n_{c_2}/kT) \quad (3a)$$

where the summation is over all n_{c_1} 's and n_{c_2} 's, which are the number of molecules in conformations c_1 and c_2 , and μ_1 and μ_2 are the chemical potentials of the two types of chains with respect to appropriate reference states, which are chosen to be pure short and long chains, respectively. The canonical partition function, Q , is defined relative to these reference states as

$$Q(\{n_{c_1}\}, \{n_{c_2}\}, M, L, T) = (\Omega / [\Omega_1 \Omega_2]) \exp(-U/kT) \quad (3b)$$

Ω is the number of ways of arranging n_1 molecules of length r_1 and n_2 molecules of length r_2 on an interfacial lattice of ML sites. Ω_1 (Ω_2) (the combinatorial factor for the reference state) is the number of ways of arranging n_1 (n_2) molecules of length r_1 (r_2) on an unconstrained lattice of $n_1 r_1$ ($n_2 r_2$) sites. U is the potential energy of the system relative to the reference states and is independent of the conformations of the chains in the case of a lattice completely filled with identically interacting chains.

The coordination number, or the number of nearest neighbors, for any site in the lattice is denoted by Z . Let

us define δ_{j-i} as the fraction of nearest neighbors in layer j available to any site in layer i . Now the different values δ_{j-i} can assume for a site in i

$$\begin{aligned} \delta_{j-i} &= \delta_0, \quad j = i \\ &= \delta_1, \quad j = i \pm 1 \\ &= 0, \quad \text{otherwise} \end{aligned} \quad (4)$$

On the basis of the above definitions, the following normalization conditions must be fulfilled:

$$\sum_{j=1}^M \delta_{j-i} = 1 \quad 1 < i < M \quad (5a)$$

$$= 1 - \delta_1 \quad i = 1, M \quad (5b)$$

since layers 1 and M (the solid surfaces) are boundaries that the polymer chains cannot penetrate. There are several possible arrangements of segments in any given conformation c_i . Following Scheutjens and Fleer,²⁰ this number can be calculated to be

$$L(Z\delta_{j-i})(Z\delta_{k-j})(Z\delta_{l-k}) \dots (Z\delta_{m-p}) \equiv LZ^{r-1}w_{c_i} \quad (6)$$

If n_{c_1} and n_{c_2} denote the number of chains in conformations c_1 and c_2 , respectively, one can then write the mass balance equation

$$\sum_{c_1} n_{c_1} + \sum_{c_2} n_{c_2} = n_1 + n_2 = N \quad (7)$$

If $r_{1,i c_1}$ and $r_{2,i c_2}$ denote the number of segments of the chains in layer i belonging to conformations c_1 and c_2 , the condition for total occupancy is

$$L = \sum_{c_1} r_{1,i c_1} n_{c_1} + \sum_{c_2} r_{2,i c_2} n_{c_2} \quad \forall i \quad (8)$$

Under these assumptions and definitions, the number of ways in which all the chains in the system can be arranged on the lattice is (see Appendix 1)

$$\Omega = (Z/L)^{[ML-N]} (L!)^M \prod_{c_1} (w_{c_1})^{n_{c_1}} / n_{c_1}! \prod_{c_2} (w_{c_2})^{n_{c_2}} / n_{c_2}! \quad (9)$$

For the reference states the combinatorial factors Ω_1 and Ω_2 are given by Flory's expression for monodisperse solutions.²⁴

$$\Omega_l = [(r_l n_l)! / n_l!] [Z / r_l n_l]^{(r_l - 1)n_l} \quad l = 1, 2 \quad (10)$$

Since the two different chains are made up of the same kind of repeat units, it is assumed that there will be identical energetic interactions between all segments and also between the segments and the surface. Thus, the potential energy of the interfacial system relative to the reference states is given by

$$U = (n_{1,1} + n_{1,M} + n_{2,1} + n_{2,M}) U_s \quad (11)$$

where U_s is the adsorption energy per polymer segment, independent of chain length.

2.2. Minimization of Grand Potential. Since the grand potential, F , is given by $-kT \ln G$, the condition for the system to be in equilibrium is that $\ln G$ should be a maximum subject to the constraints given by eq 8. The constraints (eq 8) are incorporated into the equation for the grand potential by a set of M Lagrange multipliers, m_i (one for each layer), so that the condition of equilibrium states that the function F shown below has an unconstrained stationary point.

$$F = \ln G - \sum_i m_i \left(\sum_{c_1} r_{1,ic_1} n_{c_1} + \sum_{c_2} r_{2,ic_2} n_{c_2} - L \right) \quad (12)$$

Note should be made that the summation in the calculation of G will be replaced by its largest term in eq 12, a restatement of the mean-field approximation. The extremization performed with respect to the two variables n_{c_1} and n_{c_2} yielded the following results (see Appendix 2):

$$\begin{aligned} (n_{c_1}/L) &= k_1 w_{c_1} \prod_i \{ \exp(-m_i - [\delta_{1i} + \delta_{M1}] U_s) \}^{r_{1,ic_1}} \\ &= k_1 w_{c_1} \prod_i \{ P_i \}^{r_{1,ic_1}} \end{aligned} \quad (13)$$

$$\begin{aligned} (n_{c_2}/L) &= k_2 w_{c_2} \prod_i \{ \exp(-m_i - [\delta_{1i} + \delta_{M1}] U_s) \}^{r_{2,ic_2}} \\ &= k_2 w_{c_2} \prod_i \{ P_i \}^{r_{2,ic_2}} \end{aligned} \quad (14)$$

P_i is defined to be the "free segment probability"²⁰ in layer i and assumes the same value for the two different chain lengths. k_1 and k_2 are constants that depend upon chain length, lattice parameters, and the chemical potentials of the chains (see Appendix 2). δ_{1i} (δ_{Mi}) is the Kronecker delta. Equations 13 and 14 are arithmetic expressions for the number of molecules of the two species in any given conformation when the system is in equilibrium. This is also the unnormalized probability of the occurrence of a conformation and accounts for the connected nature of the polymer molecules and the fact that it is the magnitudes of the free segment probabilities in any given conformation that define the probability of occurrence of that conformation.

We define p_i to be the free segment probability, P_i , normalized with respect to its bulk value, P_b . Then

$$p_i = P_i/P_b = \exp(-[m_i - m_b] - [\delta_{1i} + \delta_{M1}] U_s) \quad (15)$$

where m_b is the corresponding Lagrange multiplier in the bulk. We can then show that the volume fractions of the two species in layer i can be expressed as (see Appendix 3)

$$\Phi_{1,i} = [\Phi_{1b}/r_1] (1/p_i) \sum_{s_1=1}^{r_1} p(i, s_1) p(i, r_1 - s_1 + 1) \quad (16)$$

$$\Phi_{2,i} = [\Phi_{2b}/r_2] (1/p_i) \sum_{s_2=1}^{r_2} p(i, s_2) p(i, r_2 - s_2 + 1) \quad (17)$$

where Φ_{1b} and Φ_{2b} are the corresponding volume fractions in the bulk. $p(i, s)$ is termed as the normalized end segment probability and is equal to the free segment probability, p_i , for $s_i = 1$. For other values of s_i it can be calculated from the recurrence relation²⁰

$$p(i, r_l) = \sum_j \delta_{j-i} p_l(j, r_l - 1) \quad l = 1, 2 \quad (18)$$

Since the completely filled lattice is composed of only the two chain length species

$$\Phi_{1,i} = 1 - \Phi_{2,i} \quad (19)$$

Substituting eq 19 in eq 16 and eliminating $\Phi_{2,i}$ between eqs 16 and 17, one can show that

$$\begin{aligned} p_i - [\Phi_{1b}/r_1] \sum_{s_1=1}^{r_1} p(i, s_1) p(i, r_1 - s_1 + 1) - \\ [\Phi_{2b}/r_2] \sum_{s_2=1}^{r_2} p(i, s_2) p(i, r_2 - s_2 + 1) = 0 \end{aligned} \quad (20)$$

Equation 20 is a set of M simultaneous equations implicit

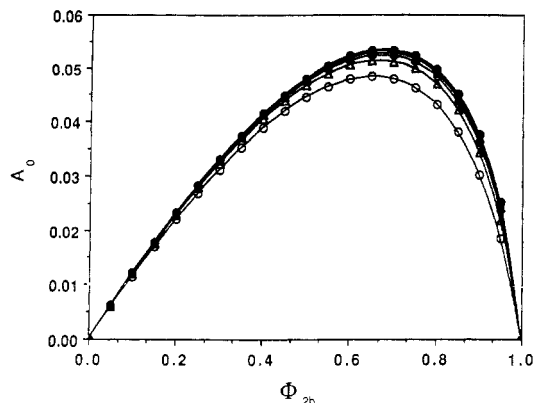


Figure 1. A_0 as a function of Φ_{2b} for a constant value of $r_2 = 10$. r_1 assumes values of 160 (○), 320 (△), 480 (□), 640 (▲), 800 (■), and 960 (●).

in p_i . Solving for the free segment probabilities in each layer enables the calculation of the segment densities in every layer using eqs 16 and 17. By analogy, eq 20 will assume a similar form for a polydisperse melt. The computations in this work, however, have been performed for a bimodal melt. The numerical procedures utilized are described in Appendix 4.

3. Results and Discussion

3.1. Segment Density Distributions. The segment density of the shorter chains $\Phi_{2,i}$ in layer i for a system with fixed chain lengths and bulk volume fractions was computed and confirmed that the shorter chains segregated to the surface due purely to entropic effects.

The concentration of the segments of the shorter chain in the interface was found to be maximum on the surface and approached its bulk value at distances characteristic of each system. This suggested that its concentration profile could be described by a functional form of the type

$$\Phi_{2,i} - \Phi_{2b} = (\Phi_{2,0} - \Phi_{2b}) f(i/\tau) \quad (21)$$

or

$$A_i = A_0 f(i/\tau) \quad (22)$$

where $A_i = \Phi_{2,i} - \Phi_{2b}$ is defined to be the absolute enhancement of the segments of the shorter chain in layer i and $i = 0$ denotes the solid surface. τ is a correlation length that characterizes the width of the interface. In the above profile, the boundary conditions for $f(i/\tau)$ are

$$f(i/\tau) = 1 \quad i = 0 \quad (23a)$$

$$= 0 \quad i = \infty \quad (23b)$$

implying that A_i takes the value A_0 on the surface (eq 23a) and is 0 far away from the surface (eq 23b). Hence, with a given set of τ and A_0 and a functional form of f , we can describe the concentration profiles of the two species in the interface completely. It should be emphasized that the form for the concentration profiles of the two species in the interface is not new since it has been previously suggested by several workers who have studied the behavior of polymer blends in the vicinity of surfaces.¹⁷

In order to delineate the profiles that have been referred to in eq 22, we begin by analyzing the absolute enhancement at the surface, A_0 . For any ratio of molecular weights, A_0 assumes a value of 0 for monodisperse systems (Φ_{2b} being equal to 0 and 1, respectively), in which case there is no segregation due to entropic effects. The behavior of A_0 is continuous between these extremes in composition as shown in Figure 1. As can be seen, the

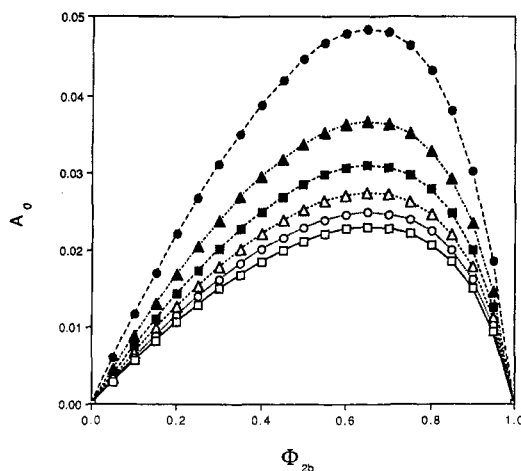


Figure 2. A_0 as a function of Φ_{2b} for increasing r_1 and r_2 while the ratio $r_1/r_2 = 16$ is kept constant. The different chain lengths used were $r_1/r_2 = 160/10$ (●), $320/20$ (▲), $480/30$ (■), $640/40$ (△), $800/50$ (○), and $960/60$ (□).

curve assumes the shape of a skewed parabola with a maximum at a certain value of Φ_{2b} that is always larger than 0.5 in our definition of the components 1 and 2. Evidently, as the molecular weight of the longer chain is decreased, the maximum value of the absolute enhancement on the surface occurs at lower values of Φ_{2b} , thus diminishing the skewness of the curve. The skewness is thus representative of the disparity in the chain lengths of the two species comprising the system.

The segregation of the shorter chains to the surface is, as explained before, a purely entropic effect. Consequently the shorter chains are thermodynamically driven to the surface so as to maximize the entropy of the system. The magnitude of A_0 is thus one measure of the net entropic loss experienced by the interfacial system. Therefore, if one increases the degree of polymerization (DP) of the longer chain while keeping the shorter chain of constant DP, A_0 will increase, reasserting the entropic nature of the segregation. This aspect of the results is clearly illustrated in Figure 1.

Finally, A_0 proceeds toward an asymptotic value as the DP of the longer chain is increased toward infinity. This suggests that A_0 , the enrichment at the surface, does not completely describe the effects of a purely entropic barrier on the thermodynamics of such an interfacial system since it is to be expected that the interface will be broadened as one increases the DP of the longer chain, while leaving that of the shorter chain unchanged. A further discussion of this aspect of the work is deferred to the latter part of this section.

For a given ratio of molecular weights the peak in A_0 , however, does not shift with respect to the abscissa. This can be seen in Figure 2, which is a plot of surface segregation for different molecular weights of the two chains with a constant chain length ratio of 16. Here the peak occurs at the same bulk volume fraction, which corresponds to $\Phi_{2b} \approx 0.65$, in all cases. The shift in the peak position toward higher values of Φ_{2b} in Figure 1 (which was concluded to be suggestive of disparity in chain lengths) is thus representative of a disparity in the chain lengths of the two species as measured by the ratio of their DP's. The absolute enhancement on the surface, however, becomes smaller for the higher molecular weights, corresponding to the same ratio and again proceeds to an asymptotic value. The order of magnitude of the segregation on the surface is 1–10% of the bulk composition, reaching the maximum value at low molecular

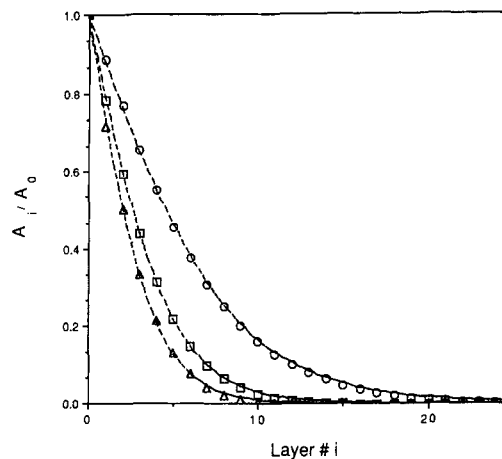


Figure 3. Normalized concentration profiles of the segments of the shorter chain and the corresponding hyperbolic tangent profiles (dashed lines) for systems composed of chain lengths 800 and 50. The three curves correspond to various bulk volume fractions of the shorter chain: 0.1 (▲), 0.5 (□), and 0.9 (○).

weights. It is thus noted that the surface enhancement due to entropic effects in a truly macromolecular system is small, typically of the order of 1 vol % or less.

Concentration profiles depicting the rate of decay from the surface for a system composed of chain lengths 800 and 50 at three different values of Φ_{2b} (0.1, 0.5, and 0.9) are shown on Figure 3. The quantity that is plotted is A_i/A_0 versus the distance from the surface (layer number). Among many functions that satisfy the boundary conditions eq 23, a hyperbolic tangent function was found to be most appropriate. It is represented as

$$f(i/\tau) = 1 - \tanh(i/\tau) \quad i = 0, 1, \dots, \infty \quad (24)$$

The agreement between the lattice model predictions and the suggested profile (eq 24), as can be seen in Figure 3, is excellent. The hyperbolic tangent profile was found to reproduce the lattice results accurately for all the bimodal systems that were studied in this work.

The correlation lengths, τ , which represent one measure of the size of the interface, assumed values, in all cases, that were intermediate between the radii of gyration of the two chains. The effect of the increase of τ is seen from the fact that the rate of decay of the profile in Figure 3 decreases as Φ_{2b} increases. The variation of the correlation length with the bulk volume fraction of the short chain is shown in Figure 4 and was found to be described by the relationship

$$\tau^{-2} = \Phi_{2b}R_1^{-2} + \Phi_{1b}R_2^{-2} \quad (25)$$

where

$$R_l = \alpha(r_l/6)^{1/2} \quad l = 1, 2 \quad (26)$$

If the system were to behave as an ideal melt, then we expect α to assume a value of unity. However, it was found that α usually assumed a value between 1.01 and 1.2 for low and high values of the DP of the shorter chain, respectively. The reason for this discrepancy is not clear at this time. The relation suggests that the correlation length increases from R_2 (approximately the radius of gyration of the short chain) continuously as the volume fraction of the shorter chains is increased and attains a value of R_1 at the other extreme. In other words, for a system with infinitesimal amounts of short (long) chains in the melt, the interfacial decay is described by a correlation length of the order of the radius of gyration of the shorter (longer) chain.

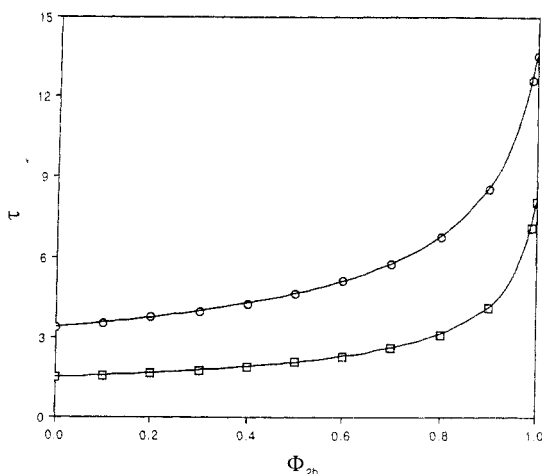


Figure 4. Behavior of the correlation lengths with the bulk volume fraction of the shorter chain segments for two systems. $\alpha = 1.14$ and 1.17 for the systems made up of chain lengths $800/50$ (O) and $300/10$ (□), respectively.

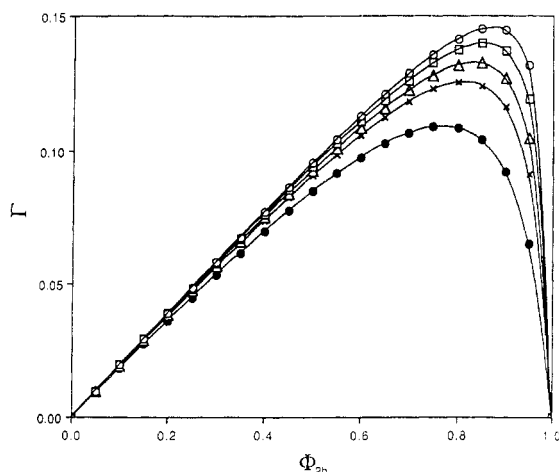


Figure 5. Γ as a function of Φ_{2b} for a constant value of $r_2 = 10$. r_1 assumes values of 160 (●), 320 (×), 480 (Δ), 800 (□), and 1440 (○).

The loss of entropy suffered by the chains due to the solid surface diminishes away from the surface and becomes insignificant at a certain distance from the surface. The correlation length, τ , reflects the magnitude of this entropic gradient created by the surface. As shown in Figure 1, A_0 reaches an asymptotic value when one increases the longer chain length for a fixed length of the shorter chain and at a constant value for bulk volume fractions of the two species. However, the correlation length of the system increases with the molecular weight of the longer chain (eq 25), followed by a corresponding increase in A_i (eq 22), thus broadening the interface. The combined effect of A_0 and τ thus describes the magnitude of the segregation completely. A measure of this quantity is the surface excess $\Gamma = \sum_i A_i$. This quantity can also be obtained by integrating eq 22 using the suggested functional form (eq 24) of the profile and was found to be equal to $A_0 \tau \ln 2$.

In Figure 5 we plot the surface excess, Γ , versus Φ_{2b} for the same systems that were studied in Figure 1. The skewness is more pronounced in all the curves than what it is in the absolute enhancement curves (Figure 1) and becomes more so with increases in the molecular weight of the longer chain. This is due to the fact that while A_0 assumes a skewed parabolic shape with an increase in Φ_{2b} , τ increases continuously with the volume fraction of the short chains in the bulk. It should be noted that the typical value of surface excess for a truly macromolecular system

is of the order of 0.01–0.2 lattice units, which corresponds to 0.1 nm or less for typical systems.

3.2. Interfacial Tension. In section 3.1 we described the structure of the interface in detail by studying the segment density distribution of the shorter chain. The motivation behind this work was to probe the modification of the physical properties of the interface formed due to the effects of polydispersity in a polymer in the vicinity of a solid surface. The quantity of interest is therefore the interfacial tension, which is a measure of the extent of adhesion of the polymer on the substrate.

The interfacial free energy at equilibrium can be calculated from the grand canonical partition function (eq 3a) as

$$fa/kT = -1/L \ln (G/G^b) \quad (27a)$$

Here, f is the interfacial tension, a is the area per site on the surface, G is the grand canonical partition function for the interfacial system, and G^b is the grand partition function for the bulk system. However, since G^b is equal to unity, it can be shown that

$$fa/kT = -1/L(\ln Q + n_1\mu_1 + n_2\mu_2) \quad (27b)$$

μ_1 and μ_2 are the chemical potentials of the two different chains and can be derived from G^b . The resulting expressions for the chemical potentials are the same as Flory's result for the polymers in multicomponent solutions.²⁴

$$\mu_1 = \Phi_{2b} + \ln(\Phi_{1b}) - (r_1/r_2)\Phi_{2b} \quad (28a)$$

$$\mu_2 = \Phi_{1b} + \ln(\Phi_{2b}) - (r_2/r_1)\Phi_{1b} \quad (28b)$$

Equation 27b can then be simplified to

$$fa/kT = U_s/kT + \sum_i \{\ln p_i + A_i(r_1^{-1} - r_2^{-1})\} \quad (29)$$

Substituting the profile eq 22 in this equation yields

$$fa/kT = U_s/kT + \sum_i \ln p_i + A_0(r_1^{-1} - r_2^{-1}) \sum_i f(i/\tau) \quad (30a)$$

$$= U_s/kT + \sum_i \ln p_i + A_0(r_1^{-1} - r_2^{-1}) \tau \ln 2 \quad (30b)$$

The first term is the energetic contribution and the latter two are the entropic terms. The first entropic term is a function of the free segment probability in each layer, and its effect, therefore, is due to the modification of p_i as the length and amount of the shorter chains in the system vary. In this term, p_i reaches a value close to the bulk value of 1 after the second lattice layer (see Figure 6) and hence the contribution from this term is mainly from the surface layer. The second entropic term (third term in eq 30) represents the effect of the disparity in sizes and entropic segregation and is proportional to Γ . For a monodisperse system, this term goes to 0 and the surface tension goes to the appropriate value for a pure monodisperse polymer as reported in ref 23. This contribution is negative and is responsible for lowering the surface tension. For a given set of molecular weights, the two contributions add up (Figure 7a,b), so that the surface tension now varies linearly with Φ_{2b} as shown in Figure 7c. Note must be made that the two parts are not independent of each other since the surface excess term depends on the free segment probability as can be seen from eqs 16 and 17. It was found that the surface tension calculated from the lattice theory could be reproduced accurately by a relationship

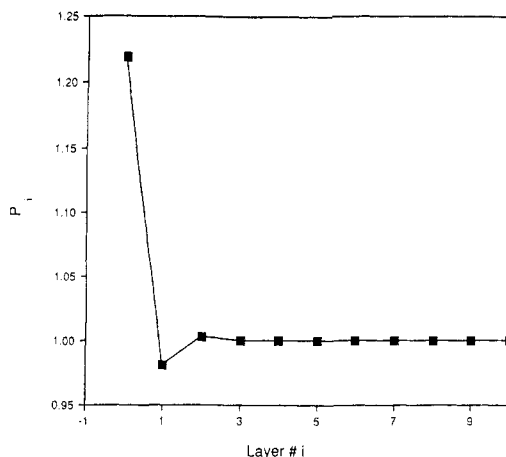


Figure 6. Profile of the normalized free segment probability p_i . The bimodal melt was composed of chain lengths 160/10 and had equal amounts of each species in the bulk.

$$fa/kT = 0.1934(1 - \Phi_1 r_1^{-1} - \Phi_2 r_2^{-1}) - 0.0092 \quad (31a)$$

or

$$fa/kT = 0.1934(1 - X_n^{-1}) - 0.0092 \quad (31b)$$

where X_n is the number-average degree of polymerization of the bimodal melt.

A plot of the reduced surface tension (fa/kT) versus the inverse chain length of the shorter chain for a given longer chain length (Figure 8) shows the agreement between the lattice results and the above equation. Also, for a given set of chain lengths, the surface tension proceeds linearly with volume fraction, as suggested by the above relation; this can be seen in Figure 7c. The surface tension of a bimodal melt on the surface is thus shown to be a simple weighted average of the values corresponding to the two monodisperse systems comprising the melt. From eq 31b one can see that the surface tension depends only on the number-average molecular weight of the melt under consideration. The discrepancy in chain lengths and the relative amounts of each of the species are thus the important factors affecting the surface tension of the bimodal melt.

3.3. Bond Orientation Characteristics. It has been shown by Theodorou²³ that the interfacial thickness defined with respect to ordering is quite insensitive to molecular weight in the case of monodisperse systems. We examine the same effect for the bimodal melt under consideration by studying the order parameter of segment orientation S_{li} ($l = 1, 2$) of the chains. The order parameter S_{li} for the segments of chains of type l in any layer i is given by²³

$$S_{li} = (3\langle \cos^2 \theta \rangle - 1)/2 = 1.0 - 1.5q_{li} \quad (32)$$

where q_{li} is the average side-stepping probability and is the ratio of the probability of two consecutive segments lying on a layer i to the probability of one of the r_l first segments lying in the same layer i ; θ is the average angle made by a segment with respect to the normal to the surface. From ref 23

$$q_{li} = \frac{\delta_0 p_i \sum_{s_l=1}^{r_l-1} p(i, s_l) p(i, r_l - s_l)}{\sum_{s_l=1}^{r_l-1} p(i, s_l) p(i, r_l - s_l + 1)} \quad (33)$$

From eq 32 it can be seen that for chains absolutely

perpendicular (parallel) to the surface, s_{li} should be 1 (~ 0.5), and for randomly oriented chains it takes the value 0.

The changes in bond order in the interface from the case of a pure homopolymer to a bimodal melt were seen to be negligible in our calculations. The segments of the longer (shorter) chains did not display any significant changes in bond order when the amounts and lengths of the shorter (longer) chain were allowed to vary. The inclination for perpendicularity in the first layer that was observed in monodisperse systems^{1,23} is maintained (see Figure 9) but with almost no significant changes in the extent of orientation as the melt is perturbed by varying the amount of chains of a different length. Bond orientation thus does not seem to be affected by perturbation of a monodisperse system by a species of a different chain length in varying proportions.

4. Conclusions

In this work we have calculated, with the aid of a quasi-crystalline lattice model, the segregation of shorter chains to a surface from a bimodal melt composed of shorter and longer chains with given bulk composition. Only entropic effects have been considered, and it is assumed that the beads of the polymer chains have no energetic interaction with other beads. In addition, all beads of both the chain length species have the same energy of interaction with the surface. Under these assumptions it was found that purely entropic effects caused the shorter chains to partition preferentially to the neutral surface. The concentration profile for the short chains in the vicinity of the surface possessed a hyperbolic tangent functional form with a single variable, which was defined as the correlation length in the system. It was found that this correlation length depended in a very simple fashion on the radii of gyration of the two chain length polymers and also their compositions in the bulk phase.

It was determined for chains consisting of identical repeat units that entropic effects alone caused the presence of an excess quantity of shorter chains at the surface only of the order of 1% or lower in the case of a truly macromolecular system. As well be shown in a future publication,²⁵ however, if one chain were to interact energetically with the surface differently from the other species (as in the case where one chain is deuterated and the other hydrogenated), then the segregation is driven purely by energetic effects, and the chains with the lower surface energy are partitioned preferentially to the surface. Under this circumstance the segregation due purely to entropic effects is dominated by the partitioning due to energetic considerations. Thus, the segregation of chains to a surface due to entropic effects (caused by molecular weight differences) alone cannot be measured in a real experiment, since in this case one chain length species must be distinguishable from the other, a modification that could be achieved by the tagging of one species for example by deuteration.

Acknowledgment. Partial funding for this work was provided by the IBM Corp. and the donors of the Petroleum Research Fund, administered by the American Chemical Society.

Appendix 1. Number of Ways of Arranging the Bimodal Polymer Melt on the Lattice

The number of arrangements in a given conformation (eq 6) has to be corrected for previous occupancy. According to the Bragg-Williams approximation of random

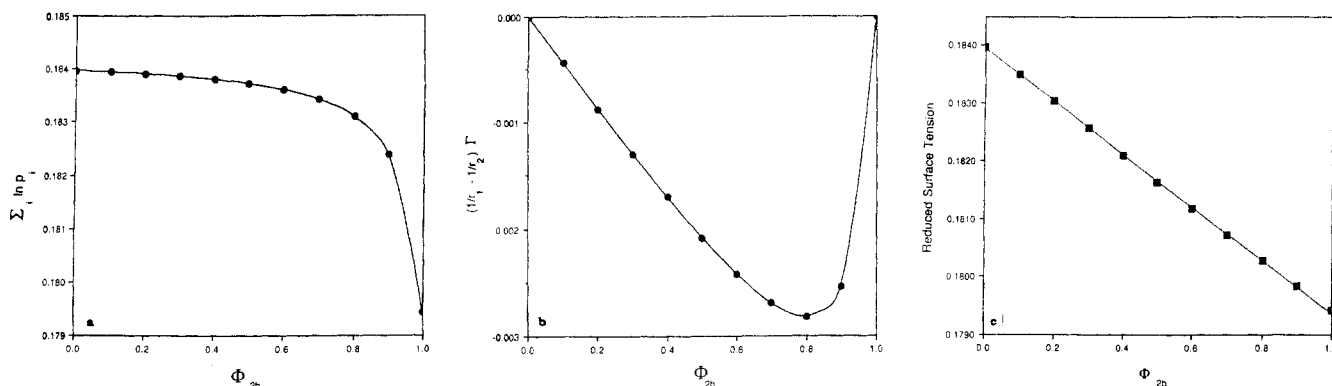


Figure 7. Variation of surface tension with bulk volume fraction of the segments of the shorter chain. The melt is made up of chains of length 800 and 40. (a) Contribution to the surface tension from the free segment probability p_i (eq 29). (b) Contribution to the surface tension from the surface excess term (eq 29). (c) The sum of the curves in (a) and (b) yields the net entropic contribution. The filled squares correspond to the lattice theory, while the line was constructed from values generated by eq 31a.

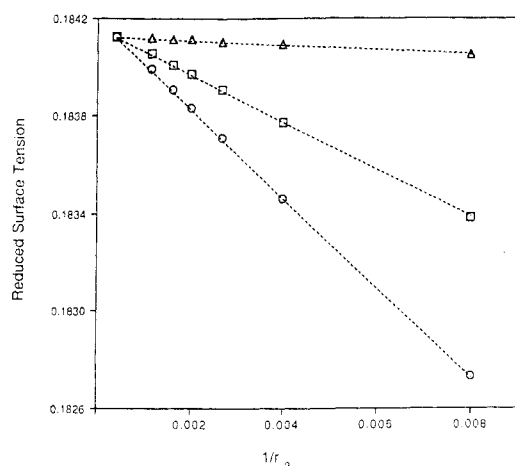


Figure 8. Surface tension plotted against inverse chain length of varying lengths of the shorter chain while the longer chain length is made up of 2500 segments. The agreement between the lattice theory (labels) and eq 31a (dashed line) is shown for systems corresponding to $\Phi_{2b} = 0.05$ (Δ), 0.5 (\square), and 0.95 (\circ).

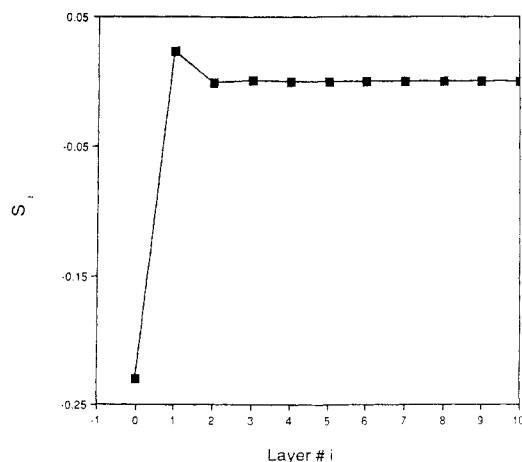


Figure 9. Order parameter profile of the segments of the shorter chain of a system composed of chain lengths 160 and 10. $\Phi_{2b} = 0.5$.

mixing, for v_i previously occupied sites in a layer i , any site in that layer has a vacancy probability equal to $(1 - v_i/L)$. The number of arrangements of a molecule in a conformation c_1 can now be written as

$$Lw_{c_1}Z^{r-1} \prod_{i=1}^M \prod_{j=1}^{r_{1,jc_1}-1} (1 - v_i/L) \quad (\text{A1.1})$$

The number of ways, $w(n_1)$, of placing n_{c_1} chains of length

r_1 in the same conformation c_1 is given by eq 10 being multiplied by itself n_{c_1} times.

$$w(n_1) = (w_{c_1})^{n_{c_1}} (Z/L)^{(r_1-1)n_{c_1}} \prod_{i=1}^M \prod_{j=1}^{r_{1,jc_1}-1} (L - v_i) \quad (\text{A1.2})$$

The number of ways of arranging all the n_1 chains over all possible conformations is given by the product of $w(n_1)$ over c_1, d_1, e_1, \dots , etc.

$$W_1 = \prod_{c_1} w(n_1) = (Z/L)^{(r_1-1)n_1} \prod_{c_1} (w_{c_1})^{n_{c_1}} \prod_{i=1}^M \prod_{j=1}^{r_{1,j}-1} (L - v_i) \quad (\text{A1.3})$$

On this partially filled lattice, the chains of length r_2 are placed so that

$$W_2 = \prod_{c_2} w(n_2) = (Z/L)^{(r_2-1)n_2} \prod_{c_2} (w_{c_2})^{n_{c_2}} \prod_{i=1}^M \prod_{j=1}^{L-1} (L - v_i) \quad (\text{A1.4})$$

Finally, the number of ways of arranging the N chains on the ML lattice sites is given by $\Omega = W_1 W_2$ or

$$\Omega = (Z/L)^{(r_1-1)n_1 + (r_2-1)n_2} \prod_{c_1} (w_{c_1})^{n_{c_1}} / n_{c_1}! \times \prod_{c_2} (w_{c_2})^{n_{c_2}} / n_{c_2}! \prod_{i=1}^M \prod_{j=1}^{L-1} (L - v_i) \quad (\text{A1.5})$$

Division by $n_{c_1}!$ and $n_{c_2}!$ has been done to correct the counting for indistinguishability of the molecules of a particular chain length. Substituting eqs 1 and 7 in eq A1.5, we get eq 9.

Appendix 2. Minimization of the Grand Potential of the Lattice System

Let us define for convenience

$$[d/dn_{c_1}]_{M,L,T,n_{c_2},n_{d_1} \neq n_{c_1}} = (d/dn_{c_1}) \quad (\text{A2.1})$$

$$(d/dn_{c_2})_{M,L,T,n_{c_1},n_{d_2} \neq n_{c_2}} = (d/dn_{c_2}) \quad (\text{A2.2})$$

The population balance on each layer i is

$$n_{i,l} = \sum_{c_1} r_{l,jc_1} n_{c_1} \quad l = 1, 2 \quad (\text{A2.3})$$

By differentiation of eq 1 with respect to n_{c_1} and n_{c_2} , the following set of relationships can be derived.

$$d/dn_{c_1}(n_1) = d/dn_{c_2}(n_2) = 1 \quad (\text{A2.4})$$

$$d/dn_{c_1}(n_2) = d/dn_{c_1}(\sum_{c_2} n_{c_2}) = -r_1/r_2 \quad (\text{A2.5})$$

$$d/dn_{c_2}(n_1) = d/dn_{c_2}(\sum_{c_1} n_{c_1}) = -r_2/r_1 \quad (\text{A2.6})$$

Substituting eqs 3 and 11 in eq 12, after simplification,

yields

$$F = (n_1 + n_2) \ln(L) - n_1 \ln(r_1) - n_2 \ln(r_2) - \sum_{c_1} n_{c_1} \{ \ln(n_{c_1}/w_{c_1}) + \sum_i m_i r_{1,ic_1} \} - \sum_{c_2} n_{c_2} \{ \ln(n_{c_2}/w_{c_2}) + \sum_i m_i r_{2,ic_2} \} + (\mu_1 \sum_{c_1} n_{c_1} + \mu_2 \sum_{c_2} n_{c_2}) / kT - (n_{1,1} + n_{2,1}) U_s / kT - L \sum_i m_i \quad (\text{A2.7})$$

Operating eqs A2.1 and A2.2 on eq A2.7 by making use of eqs A2.3–A2.6, we get eqs 13 and 14, in which

$$k_1 = (1/r_1 e)(L)^{1-r_1/r_2} r_1/r_2 e^{(1/kT)(\mu_1 - [r_1 \mu_2 / r_2])} \quad (\text{A2.8})$$

$$k_2 = (1/r_2 e)(L)^{1-(r_2/r_1)} r_2/r_1 e^{(1/kT)(\mu_2 - [r_2 \mu_1 / r_1])} \quad (\text{A2.9})$$

Appendix 3. Expression for Volume Fractions of the Two Species in a Layer as Functions of the Free Segment Probabilities

The conformation probability of species l ($l = 1, 2$) is

$$P(r_l)_{c_l} = w_{c_l} \prod \{P_{ij}\}^{r_{l,ic_l}} \quad l = 1, 2 \quad (\text{A3.1})$$

and the chain probability is defined as

$$P(r_l) = \prod_{c_l} P(r_l)_{c_l} \quad l = 1, 2 \quad (\text{A3.2})$$

Using the Scheutjens and Fleer formalism²⁰ for the two chain species ($l = 1, 2$) now gives us

$$\Phi_{l,j} = [n_l / LP(r_l)] (1/P_l) \sum_{s_l=1}^{r_l} P(i, s_l) P(i, r_l - s_l + 1) \quad (\text{A3.3})$$

where the end segment probability $P(i, s_l)$ can be generated from the recurrence relation

$$P(i, r_l) = \sum_j \delta_{j-i} P_i P(j, r_l - 1) \quad (\text{A3.4})$$

The normalized end segment probability and chain probability are defined, respectively, as

$$p(i, r_l) = P(i, r_l) / P_b^{r_l} \quad (\text{A3.5})$$

$$p(r_l)_{c_l} = P(r_l)_{c_l} / P_b^{r_l} \quad (\text{A3.6})$$

Applying eq A3.3 in the bulk of the melt gives

$$\Phi_{lb} = n_l r_l / LP(r_l) \quad (\text{A3.7})$$

Substituting eq A3.7 in eq A3.3 while using the normalization conditions stated by eqs 15, A3.5, and A3.6 yields eqs 16 and 17. Also, dividing eqs 13 by their summations over all conformations c_l results in

$$(n_{c_l} / n_l) = w_{c_l} (\prod \{P_{ij}\}^{r_{l,ic_l}} / P(r_l)) \quad l = 1, 2 \quad (\text{A3.8})$$

Using eqs A3.5–A3.7 in eq A3.8 gives

$$n_{c_l} / L = (w_{c_l} \varphi_{lb} / r) \prod \{p_{ij}\}^{r_{l,ic_l}} \quad l = 1, 2 \quad (\text{A3.9})$$

Appendix 4. Solution of the Free Segment Probabilities

The end segment probabilities were generated by representing eq 18 as a product of matrices

$$\mathbf{p}(r_1) = \mathbf{w} \mathbf{p}(r_1 - 1) \quad (\text{A4.1})$$

where $\mathbf{p}(r_1)$ and $\mathbf{p}(r_1 - 1)$ denote one-dimensional vectors with M rows containing the end segment probabilities $p(i, r_1)$ and $p(i, r_1 - 1)$. \mathbf{w} is given by

$$\mathbf{w} = \begin{bmatrix} \delta_0 p_1 & \delta_1 p_1 & 0 \\ \delta_1 p_2 & \delta_0 p_2 & \delta_1 p_2 \\ \vdots & \vdots & \vdots \\ \delta_1 p_i & \delta_0 p_i & \delta_1 p_i \\ \vdots & \vdots & \vdots \\ \delta_1 p_{M-1} & \delta_0 p_{M-1} & \delta_{M-1} p_{M-1} \\ 0 & \delta_1 p_M & \delta_0 p_M \end{bmatrix} \quad (\text{A4.2})$$

The end segment probabilities of the longer chain were stored in an array f_1 of size $M \times r_1$ sequentially. By virtue of eqs 13 and 14, the end segment probabilities corresponding to the second chain are the elements in the first r_2 columns of f_1 . \mathbf{w} was stored in an $M \times 3$ array, and due to the inherent symmetry of the problem about the middle layer, the available computational space was doubled. Convergence was always obtained by starting with an initial guess of p_i ($i = 1, M$) = (1.2, 1.1, 1.1, ...).

Notation

English

a	area per segment
A_i	absolute enhancement of segments of short chains in layer i
c_l	any conformation of a chain of type l
f	function describing the concentration profile of short chains in the interface
f	interfacial tension
G	grand canonical partition function
k	Boltzmann's constant
L	number of lattice sites in a lattice layer
m_i	Lagrange multiplier in layer i
M	number of lattice layers
n_i	number of chains of type l
$n_{l,i}$	number of segments of type l in layer i
n_{c_l}	number of chains conformation c_l
N	total number of chains
p_i	normalized free segment probability in layer i
$p(i, r_l)$	normalized end segment probability of a chain of length r_l
P_i	unnormalized free segment probability in layer i
Q	canonical partition function
r_l	number of segments in a single chain of type l
r_{l,ic_l}	number of segments of the chain of type l in layer i in conformation c_l
R_l	factor proportional to the radius of gyration of a chain of DP r_l
S_l	conformation of a chain of type i
$S_{l,i}$	order parameter in layer i of the segments of chains of type l
T	temperature
U	potential energy of the interfacial system with respect to the reference states
U_s	adsorption energy of a segment of any chain
X_n	number-average degree of polymerization
Z, z	lattice coordination number (=6)

Greek

α	constant (eq 26)
δ_{j-i}	fraction of nearest neighbors for any site in layer j in layer i
δ_{li}	Kronecker delta
μ_i	chemical potential of species i relative to the reference state
τ	correlation length of the concentration profiles of the two species

- $\Phi_{l,i}$ volume fraction of species l in layer i
 Ω combinatorial factor for the interfacial system
 Ω_l combinatorial factor for the reference system containing chains of type l

Subscripts and Superscripts

- b bulk properties
 i, j layer numbers i, j
 l denotes species type under consideration in the bimodal melt; $l = 1$ denotes the longer chain, $l = 2$ the shorter chains

References and Notes

- (1) Kumar, S. K.; Vacatello, M.; Yoon, D. Y. *J. Chem. Phys.* **1988**, *89*, 5206.
- (2) Rondelez, F.; Aussere, D.; Hervet, H. *Annu. Rev. Phys. Chem.* **1987**, *38*, 317.
- (3) Russell, T. P.; Karim, A.; Mansour, A.; Felcher, G. P. *Macromolecules* **1988**, *21*, 1890.
- (4) Bouchad, E.; Farnoux, B.; Sun, X.; Daoud, M.; Jannink, G. *Eur. Phys. Lett.* **1986**, *2*, 315.
- (5) Anastasiadis, S. H.; Gancarz, I. C.; Koberstein, J. T. *Macromolecules* **1988**, *21*, 2980.
- (6) Simha, R.; Frisch, H. L.; Eirich, F. R. *J. Phys. Chem.* **1953**, *57*, 584.
- (7) Silberberg, A. *J. Phys. Chem.* **1962**, *66*, 1872; *J. Chem. Phys.* **1967**, *46*, 1105.
- (8) DiMarzio, E. A. *J. Chem. Phys.* **1965**, *42*, 2101. DiMarzio, E. A.; McCrackin, F. L. *Ibid.* **1965**, *43*, 539. Hoeve, C. A. J.; DiMarzio, E. A.; Peyser, P. *Ibid.* **1965**, *42*, 2558.
- (9) Rubin, R. J. *J. Chem. Phys.* **1965**, *43*, 2392.
- (10) Roe, R.-J. *J. Chem. Phys.* **1965**, *43*, 1591; **1966**, *44*, 4264.
- (11) Marques, C. M.; Joanny, J. F. *Macromolecules* **1989**, *22*, 1454.
- (12) Motomura, K.; Matuura, R. *J. Chem. Phys.* **1969**, *50*, 1281.
- (13) Silberberg, A. *J. Chem. Phys.* **1968**, *48*, 2835.
- (14) Hoeve, C. A. J. *J. Polym. Sci.* **1970**, *30*, 361; **1971**, *34*, 1.
- (15) DiMarzio, E. A.; Rubin, R. J. *J. Chem. Phys.* **1971**, *55*, 4318.
- (16) de Gennes, P.-G. *Macromolecules* **1981**, *14*, 1637.
- (17) Schmidt, I.; Binder, K. *J. Phys. (Les Ulis, Fr.)* **1985**, *46*, 1631.
- (18) Roe, R.-J. *J. Chem. Phys.* **1974**, *60*, 4192.
- (19) Helfand, E. *J. Chem. Phys.* **1975**, *63*, 2192; *Macromolecules* **1976**, *9*, 307.
- (20) Scheutjens, J. M. H. M.; Fleer, G. J. *J. Phys. Chem.* **1979**, *83*, 1619.
- (21) Scheutjens, J. M. H. M.; Fleer, G. J. *J. Phys. Chem.* **1980**, *84*, 178.
- (22) Scheutjens, J. M. H. M.; Fleer, G. J. *J. Polym. Sci., Polym. Phys. Ed.* **1980**, *18*, 559.
- (23) Theodorou, D. N. *Macromolecules* **1988**, *21*, 1400.
- (24) Flory, P. J. *Principles of Polymer Chemistry*; Cornell University Press: Ithaca, NY, 1953.
- (25) Kumar, S. K.; Russell, T. P., submitted for publication in *Macromolecules*.
- (26) Kumar, S. K.; Yoon, D. Y. *Macromolecules* **1989**, *22*, 3458.

Density Profile of Terminally Adsorbed Polymers

Frank D. Blum* and Brijnaresh R. Sinha†

Department of Chemistry and Materials Research Center, University of Missouri—Rolla, Rolla, Missouri 65401

Frederick C. Schwab

Mobil Chemical Company, R&D Laboratory, P.O. Box 240, Edison, New Jersey 08818

Received September 26, 1989; Revised Manuscript Received January 15, 1990

ABSTRACT: Specifically labeled terpolymers of 2-vinylpyridine, styrene, and deuterostyrene have been prepared by anionic polymerization. The deuterostyrene was deuterated in the methine position and placed either in the middle or at the end of the triblock terpolymer. The moderately low molecular weight polymers (ca. 20 000 g/mol, polydispersity ca. 1.4) were then adsorbed onto high surface area silica. The adsorption isotherm was measured from toluene solution to plateau at about 1.75 mg of polymer/m² of silica. The environment of the styrene segments in the terpolymer attached to the silica surface and swollen with toluene was probed with ²H NMR. Comparison of ²H NMR spin-lattice relaxation time, T_1 , for the adsorbed polymer to that of the polymer in solution suggests that the local concentration of styrene segments near the middle of the polymer, i.e. next to the vinylpyridine segments, is about 0.11 g/mL. The concentration of segments located at the end of the polymer is estimated to be approximately 0.048 g/mL. These experiments suggest that the polymers are extended in a good solvent for styrene to about 4 times the styrene radius of gyration. The relaxation times (T_1 and T_2) of the surface-bound polymer were closer to each other than those for the homopolymer in solution, suggesting that the dynamics are rather different than in solution.

Introduction

The use of polymers as agents for improving colloidal stability is well-known.¹⁻⁴ In the absence of significant electrostatic forces, polymers may be used to achieve

colloidal stability through entropic stabilization, based on the inability of the polymer segments on neighboring particles to pass through each other or intertwine upon close approach. A number of theoretical treatments have been used to describe the conformation of polymer molecules on solid surfaces including those based on self-consistent-field,^{5,6} scaling,⁷ or Monte-Carlo approaches.⁸ These theories have been of importance in understanding

* Author to whom correspondence should be sent.

† Present address: Union Carbide Corp., P.O. Box 8361, S. Charleston, WV 25303.